

# Screened Coulomb quantum kinetics for resonant femtosecond spectroscopy in semiconductors

Q. T. Vu, L. Bányai, and H. Haug

*Institut für Theoretische Physik, J.W. Goethe Universität Frankfurt, Robert-Mayer-Strasse 8, D-60054 Frankfurt am Main, Germany*

F. X. Camescasse, J.-P. Likforman, and A. Alexandrou

*Laboratoire d'Optique Appliquée, Ecole Polytechnique–Ecole Nationale Supérieure de Techniques Avancées, Unité Mixte de Recherche du Centre National de la Recherche Scientifique No. 7639, Centre de l'Yvette, F-91761 Palaiseau Cedex, France*

(Received 26 August 1998)

We apply the non-Markovian quantum kinetics of carrier relaxation scattering due to carrier-carrier and carrier-LO-phonon interactions to an electron-hole gas in a semiconductor excited resonantly by coherent femtosecond laser pulses. Our theory employs the full two-time-dependent random-phase approximation (RPA) screened Coulomb potential that evolves self-consistently from a bare potential to the well-known dynamically screened RPA potential for long times. The dependence on the delay time of the differential transmission spectra for a thin layer of GaAs at 15 K is calculated and measured for a 150-fs pump pulse tuned to optical transitions between the light- and heavy-hole valence bands and the conduction band, while a delayed 30-fs probe pulse is tuned to transitions between the spin-orbit split-off valence band to conduction band. The calculated spectra explain the measured ones in a broad range of delay times and for various pump frequencies and intensities qualitatively rather well. [S0163-1829(99)00304-5]

## I. INTRODUCTION

Two-beam femtosecond spectroscopy<sup>1</sup> allows one to prepare and detect the nonequilibrium time evolution of the photoexcited carriers in a regime that can no longer be described by semiclassical, Markovian kinetics. In this ultrashort time regime the kinetics is influenced by the quantum mechanical coherence of the photoexcited carriers. Due to the energy-time uncertainty relation the scattering rates are no longer governed by the golden rule, but are expressed by memory integrals over the past of the system. The resulting relaxation and dephasing kinetics of the carriers is delayed in comparison to the instantaneously effective semiclassical kinetics. The general theory of quantum kinetics, which is relevant not only for femtosecond optical experiments but also for quantum transport in nanostructures, has been described in a recent textbook.<sup>2</sup> While the quantum kinetics due to the carrier-LO phonon interaction is already well developed and successfully tested by corresponding femtosecond four-wave-mixing experiments<sup>3</sup> and more recently with coherent control,<sup>4</sup> the more involved quantum kinetics due to Coulomb carrier-carrier scattering is less developed. The buildup of screening of the Coulomb interaction by intraband scattering needs about a period of a plasma oscillation.<sup>5</sup> For times shorter than a plasma oscillation period, the Coulomb potential between the pulse-excited carriers is essentially unscreened. For this reason we used in a previous investigation<sup>6</sup> a bare Coulomb potential in order to analyze the quantum kinetics of a femtosecond pulse excited carrier system in GaAs. In the experiments of Ref. 6, the pump pulse was tuned in such a way that it excited simultaneously electrons and holes of the heavy-hole (hh) and light-hole (lh) valence bands, but not of the spin-orbit split-off (so) valence band. With sufficient spectral resolution, and thus sufficiently long pump pulses, one excites a double-peaked electron distribution in the conduction band (see Fig. 1). These electron distributions have been studied by means of a de-

layed probe pulse tuned to transitions between the so-valence band and the conduction band. Due to the use of the bare Coulomb potential approximation, the time development of the carrier distribution could only be analyzed<sup>6</sup> in a short-time interval (i.e., delays of less than about 100 fs) and for relatively low excitation densities in order to keep the plasma frequency sufficiently low.

Recently we succeeded in including in the treatment of the Coulomb quantum kinetics a fully self-consistently screened, time-dependent Coulomb potential.<sup>8</sup> On the femtosecond timescale the screened Coulomb potential becomes a function of the space and time coordinates of the two interacting particles. The two-time-dependent screened Coulomb potential obeys an integral equation in which the integral kernel is, in the random-phase approximation (RPA), given by the intraband polarization bubble. By memory saving linear programming techniques it has become possible to in-

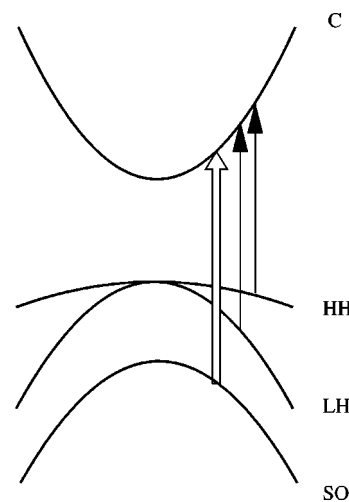


FIG. 1. Schematic diagram of the pump pulse transitions (single lines with full arrows) and the probe pulse transitions (double line).

clude a self-consistent solution of this integral equation into the numerical treatment of the semiconductor optical Bloch equations combined with the quantum kinetic relaxation and dephasing rates for the carrier-carrier scattering.<sup>8</sup>

In this paper we will present an extended application of the time-dependent screened Coulomb potential scattering to an analysis of the above described type of resonant femtosecond experiments in wider time and excitation intensity ranges, respectively. In this theory the integral equation for the two-time-dependent screened Coulomb potential is solved by expressing two-time-dependent nonequilibrium particle propagators that enter the intraband polarization by the generalized Kadanoff-Baym ansatz<sup>7,2</sup> in terms of two-time-dependent spectral functions and the reduced density matrix elements that depend on one time only. While the spectral functions are taken in the free-particle approximation, the density matrix elements are determined self-consistently by the semiconductor Bloch equations. In order to include the energy relaxation of the excited electron-hole ( $e$ - $h$ ) gas, we take in addition to the carrier-carrier scattering the scattering by LO phonons into account. We solve the semiconductor Bloch equations for the density matrix elements with these quantum kinetic scattering integrals for the various  $e$ - $h$  distributions and the interband polarization components in the presence of the strong resonant pump pulse. The differential transmission spectrum (DTS) is calculated in a simplified linear approximation by inserting the calculated electron distributions in the polarization equation for the probe pulse, which is resonant for the transitions between the so valence band and the conduction band. In this probe polarization equation the dephasing is approximated by a phenomenological density-dependent  $T_2$  time. This approximation is presently necessary because the probe polarization has to be calculated over a rather long time range in order to be able to perform a numerical Fourier transform for the calculation of the spectra. The resulting differential transmission spectra are compared with measured spectra in a wide range of delay times from  $-200$  to  $200$  fs and for the excited carrier concentration of  $4.5$  and  $8.5 \times 10^{17} \text{ cm}^{-3}$  with  $70$  and  $50$  meV excess energy, respectively. The shape of the spectra and their evolution in time are for both densities in good qualitative agreement with the observed ones.

In Sec. II we present the theoretical model for the considered four-band semiconductor, particularly the quantum kinetic scattering integrals with the time-dependent screened Coulomb potential. The Bloch equations for the pump pulse and for the delayed probe pulse with and without pump pulse are given. In Sec. III we describe the experimental setup for which we report DTS measurements on thin layer of GaAs at  $15$  K for a wide range of delay times ranging from  $-200$  to  $200$  fs and two sets of pump detuning and pump intensities, respectively. In Sec. IV we present the numerical solutions with the quantum kinetic relaxation and dephasing rates due to carrier-carrier and carrier-LO-phonon scattering, as well as the corresponding measurements. A detailed comparison shows that the calculated and measured spectra exhibit a rather similar delay time dependence and change in the same way with increasing excitation densities. Furthermore, the influence of the electron energy relaxation by LO-phonon emission on the differential transmission spectra is investigated.

## II. SEMICONDUCTOR BLOCH EQUATIONS FOR RESONANT PUMP PULSES WITH QUANTUM KINETIC SCATTERING INTEGRALS

The time-dependent system of electronic excitations in the four considered bands  $l$  will be described in terms of density matrix elements  $\rho_{l,l',\vec{k}}(t) = \langle a_{l',\vec{k}}^\dagger(t) a_{l,\vec{k}}(t) \rangle$ . The diagonal elements for  $l=e$  yield the distributions of the electrons in the conduction band  $f_{e,\vec{k}}(t)$ , while for the valence bands we replace the particle picture by the hole picture. The corresponding distributions of the holes are  $f_{\beta,\vec{k}}(t)$  with  $\beta = \text{hh, lh, so}$  for the holes in the three valence bands (see, e.g., Ref. 10). The optically active interband polarization components are  $p_{\beta,\vec{k}}(t) = \langle a_{\beta,\vec{k}}^\dagger(t) a_{e,\vec{k}}(t) \rangle e^{i\omega_\beta t}$ , where  $\omega_\beta$  is the relevant large optical frequency. Because the pulses  $E^i(t) \cos(\omega^i t)$  with  $i=p$  for the pump pulse and  $i=t$  for the test pulse excite the lh and hh transitions or the so transition, respectively, we take  $\omega_{lh} = \omega_{hh} = \omega^p$  and  $\omega_{so} = \omega^t$ . The resulting optical Bloch equations can be written in the form

$$\frac{\partial f_{e,\vec{k}}(t)}{\partial t} = \sum_{\beta} -2 \text{Im}\{\Omega_{\beta,\vec{k}}^p(t) p_{\beta,\vec{k}}^*(t)\} + \left. \frac{\partial f_{e,\vec{k}}(t)}{\partial t} \right|_{\text{scatt}},$$

with  $\beta = \text{hh, lh}$ ,

$$\frac{\partial f_{\beta,\vec{k}}(t)}{\partial t} = -2 \text{Im}\{\Omega_{\beta,\vec{k}}^p(t) p_{\beta,\vec{k}}^*(t)\} + \left. \frac{\partial f_{\beta,\vec{k}}(t)}{\partial t} \right|_{\text{scatt}},$$

$$\begin{aligned} \frac{\partial p_{\beta,\vec{k}}(t)}{\partial t} = & -\frac{i}{\hbar} \delta_{\beta,\vec{k}}^p p_{\beta,\vec{k}}(t) + i[1 - f_{e,\vec{k}}(t) - f_{\beta,\vec{k}}(t)] \\ & \times \Omega_{\beta,\vec{k}}^p(t) + \left. \frac{\partial p_{\beta,\vec{k}}(t)}{\partial t} \right|_{\text{scatt}}, \end{aligned} \quad (2.1)$$

where

$$\delta_{\beta,\vec{k}}^i = e_{e,\vec{k}}(t) + e_{\beta,\vec{k}}(t) - \Delta^i \quad (2.2)$$

is the detuning of the pulses with  $\Delta^i = \hbar \omega^i - E_G^i$ ;  $E_g^p = E_g$  is the unrenormalized energy gap for the hh and lh bands, while  $E_g^t = E_{g,so}$  is the gap of the split-off band. The Hartree-Fock renormalized Rabi frequencies are

$$\hbar \Omega_{\beta,\vec{k}}^i(t) = \frac{1}{2} d_{\beta,\vec{k}} E^i(t) + \sum_{\vec{k}'} V_{\vec{k}-\vec{k}'} p_{\beta,\vec{k}'}(t), \quad (2.3)$$

where  $d_{\beta,\vec{k}}$  is the optical matrix element for the transition between the conduction band and one of the three valence bands  $\beta = \text{hh, lh, so}$  and  $V_q = 4\pi e^2 / \epsilon_0 q^2$  is the bare Coulomb potential with the background dielectric constant  $\epsilon_0$ . Similarly, the Hartree-Fock renormalized energies are

$$e_{l,\vec{k}}(t) = \epsilon_{l,\vec{k}}^0 - \sum_{\vec{k}'} V_{\vec{k}-\vec{k}'} f_{l,\vec{k}'}(t), \quad (2.4)$$

where the index  $l=e, \beta$  designates one of the four bands. The corresponding linearized Bloch equations for the weak test pulse are with pump-excited electrons in the conduction band

$$\frac{\partial p_{so,\vec{k}}^p(t)}{\partial t} = -\frac{i}{\hbar} \delta_{so,\vec{k}}^f p_{so,\vec{k}}^p(t) + i[1 - f_{e,\vec{k}}(t)] \times \Omega_{so,\vec{k}}^t(t) + \left. \frac{\partial p_{so,\vec{k}}^p(t)}{\partial t} \right|_{scatt}, \quad (2.5)$$

and without pump pulse

$$\frac{\partial p_{so,\vec{k}}^0(t)}{\partial t} = -\frac{i}{\hbar} \delta_{so,\vec{k}}^f p_{so,\vec{k}}^0(t) + i\Omega_{so,\vec{k}}^t(t) + \left. \frac{\partial p_{so,\vec{k}}^0(t)}{\partial t} \right|_{scatt}. \quad (2.6)$$

The scattering rates are given in the framework of quantum kinetics<sup>2</sup> by

$$\begin{aligned} \left. \frac{\partial \mathcal{Q}_{\mu,\nu,\vec{k}}(t)}{\partial t} \right|_{scatt} &= \sum_{\sigma} \int_{-\infty}^t dt' [\Sigma_{\mu,\sigma,\vec{k}}^>(t,t') G_{\sigma,\nu,\vec{k}}^<(t',t) \\ &\quad - \Sigma_{\mu,\sigma,\vec{k}}^<(t,t') G_{\sigma,\nu,\vec{k}}^>(t',t) \\ &\quad - G_{\mu,\sigma,\vec{k}}^>(t,t') \Sigma_{\sigma,\nu,\vec{k}}^<(t',t) \\ &\quad + G_{\mu,\sigma,\vec{k}}^<(t,t') \Sigma_{\sigma,\nu,\vec{k}}^>(t',t)], \end{aligned} \quad (2.7)$$

where  $\Sigma^{\lessgtr}$  are the scattering self-energies of the screened Coulomb interaction between the carriers and of the interaction of the carriers with LO phonons. In equilibrium many-body theory interactions via both the Coulomb interaction and the LO phonons can be incorporated elegantly (see, e.g., Ref. 9) in an effective screened Coulomb potential. In the nonequilibrium theory the bare Coulomb potential  $V_q(t_1, t_2) = V_q \delta(t_1 - t_2)$  is singular in time, while the phonon propagator  $D_q^{\lessgtr}$  is of oscillatory nature. Because of these structural differences, we encountered difficulties in attempting to combine both interaction to an effective screened one. Therefore, we treat the scattering self-energies of both interactions additively and neglect the effect of screening for the phonon scattering. In this approximation the RPA self-energies  $\Sigma^{\lessgtr} = \Sigma_C^{\lessgtr} + \Sigma_{LO}^{\lessgtr}$  are given by

$$\Sigma_{C,\mu,\tau,\vec{k}}^{\lessgtr}(t,t') = i\hbar \sum_q G_{\mu,\tau,\vec{k}-q}^{\lessgtr}(t,t') V_{s,q}^{\lessgtr}(t,t'), \quad (2.8)$$

$$\Sigma_{LO,\mu,\tau,\vec{k}}^{\lessgtr}(t,t') = i\hbar \sum_q g_q^2 G_{\mu,\tau,\vec{k}-q}^{\lessgtr}(t,t') D_q^{\lessgtr}(t,t'), \quad (2.9)$$

with the Fröhlich interaction

$$\begin{aligned} g_q^2 &= \alpha \frac{4\pi\hbar(\hbar\omega_0)^{3/2}}{(2\mu)^{1/2}q^2}, \\ \alpha &= \frac{e^2}{\hbar} \left( \frac{\mu}{2\hbar\omega_0} \right)^{1/2} \left( \frac{1}{\epsilon_{\infty}} - \frac{1}{\epsilon_0} \right). \end{aligned} \quad (2.10)$$

Here  $\epsilon_{\infty}$  and  $\epsilon_0$  are the high- and low-frequency limits of the dielectric function of the unexcited crystal.  $\alpha$  is the dimensionless polaron constant, which for weak coupling is much smaller than one, in the intermediate coupling regime comparable to one, and for strong coupling much larger than one. The weakly polar GaAs, which will be considered here, has a

polaron constant  $\alpha = 0.069$ . For this reason we also do not consider vertex corrections here. For the interaction with the LO phonons, we consider the phonons as a thermal bath at a given temperature  $T$ ,

$$D_q^{0<}(t,t') = -i \sum_{\eta=\pm 1} e^{-i\eta\omega_0(t-t')} N_q^{\eta}, \quad (2.11)$$

$$N_q^{\eta} = \frac{1}{e^{\hbar\omega_q/kT} - 1} + \frac{1}{2} + \eta \frac{1}{2}.$$

The Keldysh components of the screened Coulomb potential are determined in the RPA by the integral equations:

$$V_q(t_1, t_2) = V_q \delta(t_1 - t_2) + V_q L_q(t_1, t_3) V_q(t_3, t_2), \quad (2.12)$$

where all time arguments lie on the Keldysh time contour extending from  $-\infty$  to  $+\infty$  and back to  $-\infty$ . The integral convention is assumed for repeated time arguments. The retarded and advanced screened Coulomb potentials can be expressed, e.g., in terms of the kinetic scattering potentials  $V_q^<$  and  $V_q^>$  by the relations

$$\begin{aligned} \begin{pmatrix} V_q^r(t,t') \\ V_q^a(t,t') \end{pmatrix} &= V_q \delta(t-t') \\ &\quad + \begin{pmatrix} \theta(t-t')[V_q^>(t,t') - V_q^<(t,t')] \\ \theta(t'-t)[V_q^<(t,t') - V_q^>(t,t')] \end{pmatrix}. \end{aligned} \quad (2.13)$$

Further symmetry relations such as  $V_q^{(\lessgtr)}(t,t')^* = -V_q^{(\lessgtr)}(t',t)$  and  $V_q^>(t,t') = V_q^<(t',t)$  allow one to calculate only the integral equation for one of the four components of the nonequilibrium potential. From Eq. (2.12) one obtains, e.g., for  $V_q^>$ , the closed equation

$$\begin{aligned} V_q^>(t,t') &= V_q \left\{ L_q^>(t,t') V_q + 2 \int_{-\infty}^t d\tau \right. \\ &\quad \times \text{Re}[L_q^>(t,\tau)] V_q^>(\tau,t') \\ &\quad \left. + 2 \int_{-\infty}^{t'} d\tau L_q^>(t,\tau) \text{Re} V_q^>(t',\tau) \right\}. \end{aligned} \quad (2.14)$$

The polarization function  $L_q^>(t_1, t_2)$  will be evaluated here in the time-dependent RPA. For a semiconductor excited with coherent light pulses, the particle propagators are matrices in the band indices

$$L_q^>(t,t') = -2i\hbar \sum_{\rho,\nu,\vec{k}'} G_{\rho,\nu,\vec{k}'+q}^>(t,t') G_{\rho,\nu,\vec{k}'}^<(t',t). \quad (2.15)$$

Note that for given polarization functions  $L_q$  in Eq. (2.14) only one integration from  $-\infty$  to  $t$  or  $t'$  is necessary, while the use of nonlinear identities such as  $V_q^< = V_q^r L_q^< V_q^a$  would include two successive time integrations, which requires much more computer memory for long-time integrations than the above described strategy. We simplify the quantum kinetics by using the generalized Kadanoff-Baym ansatz,<sup>7</sup>

which relates approximately the two-time propagators to the one-time density matrix by the relations<sup>2</sup>

$$G_{\mu,\nu,\vec{k}}^<(t,t') = -\sum_{\sigma} [G_{\mu,\sigma,\vec{k}}^r(t,t')\rho_{\sigma,\nu,\vec{k}}(t') + \rho_{\mu,\sigma,\vec{k}}(t)G_{\sigma,\nu,\vec{k}}^a(t,t')]. \quad (2.16)$$

Similarly, one can connect  $G^>(t,t')$  to  $1-\rho(t)$ . The time evolution out of the diagonal value is approximated by that of the spectral functions  $G^r(t,t')$  for  $t \geq t'$  or by  $G^a(t,t')$  for  $t \leq t'$ . These relations hold exactly in the absence of scatter-

ing and incorporate the causality correctly. In our context we approximate the spectral Green's functions  $G_{\rho,\nu,\vec{k}}^r(t,t') = G_{\nu,\rho,\vec{k}}^a(t',t)^*$  further by the damped free-particle Green's functions

$$G_{\rho,\nu,\vec{k}}^r(t,t') = -\frac{i}{\hbar} \delta_{\rho,\nu} \theta(t-t') e^{-\frac{i}{\hbar}(e_{\rho,k}-i\gamma)(t-t')}. \quad (2.17)$$

Assuming isotropy in momentum space, the quantum kinetic scattering integrals for the particle distributions  $f_{j,k}(t)$  are given by

$$\begin{aligned} \left. \frac{\partial f_{j,k}(t)}{\partial t} \right|_{scatt} &= \frac{1}{\hbar} \frac{2}{(4\pi)^2 k} \int_0^\infty dk_1^2 \int_0^\infty dq^2 \int_{t_0}^t dt' \theta \left( 1 - \left| \frac{k^2 + k_1^2 - q^2}{2kk_1} \right| \right) \text{Im} \{ f_{j,k}(t') [1 - f_{j,k_1}(t')] [V_{s,q}^>(t,t') \\ &+ g_q^2 D_q^{0>}(t,t')] + f_{j,k_1}(t') [1 - f_{j,k}(t')] [V_{s,q}^>(t,t') + g_q^2 D_q^{0>}(t,t')]^* \\ &- 2P_{j,kk_1}(t') \text{Re} [V_{s,q}^>(t,t') + g_q^2 D_q^{0>}(t,t')] \} e^{\frac{i}{\hbar}(\epsilon_{j,k} - \epsilon_{j,k_1})(t-t')} e^{-\frac{\Gamma}{\hbar}(t-t')}, \end{aligned} \quad (2.18)$$

with  $\Gamma = 2\gamma$ . The so-called p-square terms are abbreviated by

$$P_{j,k_1k_2}(t') = \begin{cases} \sum_{i=lh, hh} p_{i,k_1}(t')^* p_{i,k_2}(t'), & j=e \\ p_{j,k_1}(t')^* p_{j,k_2}(t'), & j=lh, hh. \end{cases} \quad (2.19)$$

The corresponding scattering integrals for the pump beam induced interband polarization components are for  $j=lh, hh$  given by

$$\begin{aligned} \left. \frac{\partial p_{j,k}(t)}{\partial t} \right|_{scatt} &= -\frac{i}{\hbar} \frac{1}{(4\pi)^2 k} \int_0^\infty dk_1^2 \int_0^\infty dq^2 \int_{t_0}^t dt' \theta \left( 1 - \left| \frac{k^2 + k_1^2 - q^2}{2kk_1} \right| \right) \\ &\times [ \{ [p_{j,k}(t') [1 - f_{e,k_1}(t')] - p_{j,k_1}(t') [1 - f_{j,k}(t')] [V_{s,q}^>(t,t') + g_q^2 D_q^{0>}(t,t')] \\ &+ [p_{j,k_1}(t') f_{j,k}(t') - p_{j,k}(t') f_{e,k_1}(t')] [V_{s,q}^>(t,t') + g_q^2 D_q^{0>}(t,t')]^* \} \\ &\times e^{-\frac{i}{\hbar}(\epsilon_{j,k} + \epsilon_{e,k_1})(t-t')} e^{\frac{i}{\hbar}\Delta(t-t')} e^{-\frac{\Gamma}{\hbar}(t-t')} - [k \leftrightarrow k'] ]. \end{aligned} \quad (2.20)$$

In these scattering integrals we have introduced integrals over energies, i.e.,  $k^2$  and  $q^2$ , while the angle integration resulted in the  $\theta$  functions of Eqs. (2.18) and (2.20). For the numerical evaluation we will use a discretization in energy space and not in momentum space. The latter discretization would not treat the high-energy states accurately enough. The intraband screening polarization function takes the form

$$\begin{aligned} L_q^>(t,t')|_{t>t'} &= -\frac{i}{\hbar} \frac{2}{(4\pi)^2 q} \int_0^\infty dk_1^2 \int_0^\infty dk_2^2 \theta \left( 1 - \left| \frac{q^2 + k_2^2 - k_1^2}{2qk_2} \right| \right) \\ &\times \sum_j \{ f_{j,k_1}(t') [1 - f_{j,k_2}(t')] - P_{j,k_1k_2}(t') \} \\ &\times e^{\frac{i}{\hbar}(\epsilon_{j,k_1} - \epsilon_{j,k_2})(t-t')} e^{-\frac{\Gamma}{\hbar}(t-t')}. \end{aligned} \quad (2.21)$$

Now the system of integro-differential equations for the density matrices and the screened Coulomb potential is closed.

At no point of the solution does the  $q=0$  divergence of  $V_q$  cause mathematical problems. We can show analytically that our quantum kinetic scattering integrals approach in the long-time limit the Boltzmann scattering rates calculated with a dynamically screened Coulomb potential with the Lindhard dielectric function. The frequency corresponds to the energy transfer in a collision. Before we present results of our quantum kinetic studies applied to the calculation of femtosecond time-resolved differential transmission spectroscopy we describe the experimental technique with which these spectra have been measured.

### III. EXPERIMENTAL TECHNIQUE

As already mentioned, we have used a nondegenerate pump-test scheme that allows one to isolate the electron dynamics.<sup>11,6</sup> The pump pulse excites electrons from the hh and lh valence bands, while the test pulse probes the absorption saturation of the interband transition from the so valence band to the conduction band  $c$  (see Fig. 1). Due to the large

spin-orbit splitting<sup>12</sup> in GaAs (340 meV), for not too large pump excess energies with respect to the band gap, no holes are present in the so band.

The differential absorption signal is defined as

$$-\Delta\alpha(\omega) = \alpha^0(\omega) - \alpha^p(\omega), \quad (3.1)$$

where  $\alpha^0(\omega), \alpha^p(\omega)$  denote the absorption spectra without and with a pump, respectively. It depends on the electron distribution only. Since the matrix element of the so-*c* transition is isotropic, the measured signal is equally sensitive to the presence of electrons with all possible wave-vector directions. This technique also avoids complications due to coherence effects. The advantages of the nondegenerate pump-test scheme over the different approaches that have been used to measure carrier relaxation in semiconductors such as standard pump-test experiments,<sup>13–20</sup> time-resolved photoluminescence,<sup>21,22</sup> and four-wave mixing<sup>23</sup> have been discussed in more detail in Refs. 24, 11, and 25. The laser setup consists of a Ti:sapphire mode-locked oscillator (Coherent Mira) and a 250 kHz regenerative amplifier system (Coherent RegA) pumped by a single argon-ion laser. The output of the amplifier is tunable from 760 to 860 nm and is directly used as the pump pulse with a duration of 150 fs for a 15 meV width. Part of this output generates a spectral continuum by focusing into a sapphire crystal and is used as the test pulse. After chirp compensation of the continuum with a combination of prisms and gratings in order to correct up to the third derivative of the phase, we obtain nearly Fourier-transform-limited pulses with a duration of 30 fs for the test pulse with a practically flat phase in the wavelength range of interest.

The transmitted test beam was dispersed in a 0.25-m spectrometer and detected with a charge-coupled device (CCD) detector. In order to minimize the noise, a shutter is used in the optical path of the pump and the transmitted test is detected in the presence and in the absence of the pump at an 8-Hz rate. Furthermore, a reference beam is simultaneously detected on a different track of the CCD and is used to normalize the transmitted test beam.

The sample consists of an intrinsic GaAs layer ( $d = 0.65 \mu\text{m}$ ) between two  $0.2\text{-}\mu\text{m}$   $\text{Ga}_{0.35}\text{Al}_{0.65}\text{As}$  layers grown by molecular-beam epitaxy on a GaAs substrate. The substrate was selectively etched away and antireflection coatings were deposited on both sides of the sample. Thus the reflectivity is minimized and the transmitted intensity  $I_T^p$  with and  $I_T^0$  without a pump can be directly used to obtain the differential absorption signal:

$$S_{DT}(\omega) \approx -\Delta\alpha d = \ln\left(\frac{I_T^p}{I_T^0}\right). \quad (3.2)$$

The sample is held at 15 K on the cold finger of a He-compressor cryostat.

#### IV. CALCULATED AND MEASURED DIFFERENTIAL TRANSMISSION SPECTRA

The linear absorption coefficient of the test beam is defined by

$$\alpha(\omega) = \frac{4\pi\omega}{cn(\omega)} \text{Im} \frac{P^t(\omega)}{E^t(\omega)}, \quad (4.1)$$

where the index of refraction  $n(\omega)$  will be approximated by a constant that is characteristic of the band edge refraction.

The Fourier transforms of the test beam and the test beam induced polarization are given by

$$E^t(\omega) = \int_{-\infty}^{+\infty} dt E^t(t) e^{i(\omega - \omega_t)t}, \quad (4.2)$$

$$P^t(\omega) = \int_{-\infty}^{+\infty} dt \sum_k d_k p_{so,k}(t) e^{i(\omega - \omega_t)t}.$$

Because these formula require the knowledge of the test beam induced interband polarization at all times, we will simplify the dephasing of the test beam polarization equation by using a phenomenological dephasing in the form

$$\left. \frac{\partial p_{so,k}(t)}{\partial t} \right|_{scatt} \rightarrow -\frac{1}{T_2(t)} p_{so,k}(t), \quad (4.3)$$

where

$$\frac{1}{T_2(t)} = \frac{1}{T_2^0} + \gamma n(t). \quad (4.4)$$

where  $n(t)$  is the carrier concentration excited by the preceding pump pulse and is zero without a pump pulse.

Obviously, the disadvantage of this approximation is that the pump induced linebroadening is not included accurately. However, a very long time integration of the test beam polarization equation with quantum kinetic dephasing integrals is presently not possible. We will calculate the differential transmission spectra for the following GaAs material parameters and for the pulse parameters of the experiments: exciton Bohr radius  $a_B = 120 \times 10^{-8}$  cm, exciton Rydberg  $E_0 = e^2/2\epsilon_0 a_B = 4.9$  meV, static dielectric constant  $\epsilon_0 = 12.2, m_{hh}/m_e = 6.8, m_{lh}/m_e = 1.2, m_{so}/m_e = 2.2$ , polaron constant  $\alpha = 0.069$ ; temperature  $T = 15$  K, LO-phonon energy  $\hbar\omega_0 = 36$  meV, and single-particle damping constant  $\Gamma = 1$  meV. The pump and test pulses are taken to be Gaussian  $E(t) = e^{-i\omega t} E_0 e^{-2 \ln 2 \frac{t^2}{\delta t^2}}$ , with the full widths at half maximum of  $\delta t_p = 150$  fs and  $\delta t_T = 30$  fs and for the detuning frequencies  $\Delta = \hbar\omega - E_g = 70$  and 50 meV, respectively. The strength of the field amplitude will be given in terms of the fraction  $\chi$  of a  $\pi$  pulse, i.e.,  $\int_{-\infty}^{+\infty} dt d_0 E_0(t) = \chi \pi \hbar$ . For the numerical integrations the cutoff energy for the energy summations has been taken to be  $E_{max} = 150$  meV and  $N = 45$  energy points have been taken into account. The time steps have been taken as  $\Delta t = 2$  fs.

In Fig. 2 we present the time evolution of the electron distribution generated by the pump pulse and calculated by the quantum kinetic description of the screened Coulomb and LO-phonon scattering. One sees clearly how a double peaked distribution is excited by the pump pulse due to transitions out of the hh and lh valence bands. The scattering processes redistribute the electrons and already 200 fs after the center of the pump pulse a monotonically decreasing distribution is generated that relaxes in the next 200 fs towards a thermal Fermi-like distribution. Compared to our

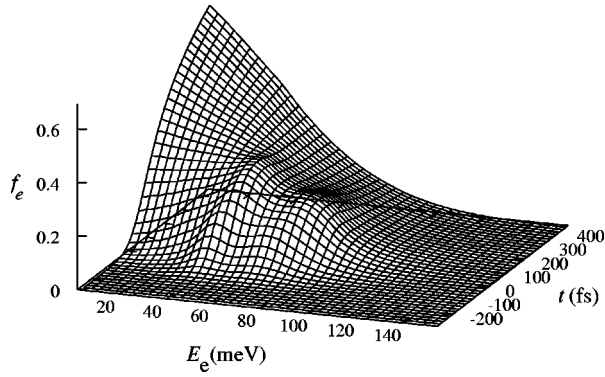


FIG. 2. Calculated electron distribution function versus electron energy and time generated by a 150-fs pump pulse with a strength of  $\chi=0.72$ , which generates the electron density  $n=4.5 \times 10^{17} \text{ cm}^{-3}$ . The detuning with respect to the unrenormalized lh-hh band gap was  $\Delta=70 \text{ meV}$ .

earlier calculations of the Coulomb quantum kinetics with bare Coulomb potential interaction,<sup>6</sup> one sees that the time-dependent screening has smoothed the resulting transient distributions.

In the lower part of Fig. 3 we present the corresponding calculated differential transmission spectra for various delay times between the pump and the test in steps of 40 fs and ranging from  $-160$  to  $200$  fs. Due to band gap renormalization and induced line broadening one sees induced absorption below the exciton resonance at the original  $E_{so,g}$ . Simi-

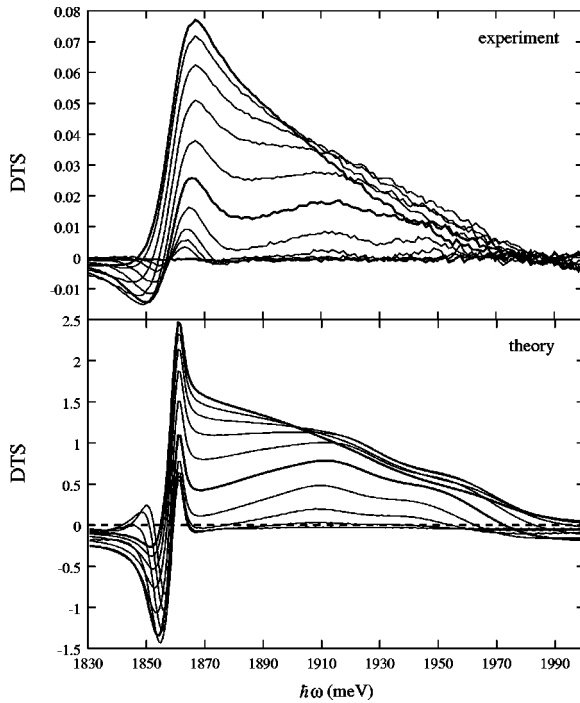


FIG. 3. Measured (top) and calculated (bottom) differential transmission spectra in GaAs at 15 K for various delay times in steps of 40 fs ranging from  $\tau=-160$  to  $200$  fs for a pump pulse with a strength of  $\chi=0.72$ , which generates the electron density  $n=4.5 \times 10^{17} \text{ cm}^{-3}$ . The central pump frequency was  $1.589 \text{ eV}$ , corresponding to a detuning with respect to the unrenormalized lh-hh band gap of  $\Delta=70 \text{ meV}$ . For the calculation of the test spectra, we used  $T_2^0=170 \text{ fs}$  and  $\gamma=0.6 \times 10^{-20} \text{ cm}^3 \text{ fs}^{-1}$ .

larly, the excitonic enhancement causes a weak induced absorption above the populated states. The double peak structure can be seen in the calculated spectra up to delay times of about 80 fs, while for larger delays, particularly with  $\tau=160$  and  $200$  fs, already monotonically decreasing distributions are reached. The corresponding measured spectra are shown at the top of Fig. 3. From the experiment we estimate carrier densities from the spectrally integrated differential absorption signal after the end of the pump pulse and from the pump excitation density and the measured linear absorption of the sample to be  $2 \times 10^{17} \text{ cm}^{-3}$  in Fig. 3 (top) and  $4 \times 10^{17} \text{ cm}^{-3}$  in Fig. 5 (top), respectively. For the best fits of the calculated spectra slightly different densities have been assumed. The experimental spectra show also the characteristic peaked structures at 1914 and 1950 meV in Fig. 3 (top) and 1898 and 1922 meV in Fig. 5 (top) corresponding to the nonequilibrium electron populations injected from the lh and hh valence bands, respectively. These structures broaden due to carrier-carrier scattering and the electrons tend to accumulate at the bottom of the conduction band due to LO-phonon emission. While the central part of the differential absorption spectrum reflects the electron distribution, the negative signal at high energies and the oscillatory signal just below the so-c band gap are not population signals. As shown by the theoretical analysis, the high-energy induced absorption can be attributed to a modification of the excitonic enhancement, while the oscillatory signal is due to the so-c exciton, which, even though it is hardly visible in the linear absorption spectrum,<sup>11</sup> gives a non-negligible differential signal. All these complicated features are extremely well reproduced by the theory.

In particular, the double-peak structure at early delay times, the induced absorption regions below and above the populated states, and the speed of the evolution of the spectra are correctly given by the theory. Due to the energy relaxation by LO-phonon emission, the present calculations predict correctly that for larger delay times there is no longer a dip in the DTS above the exciton resonance, which one would get without the phonon scattering. However, due to the oversimplified, phenomenological description of the dephasing of the test pulse polarization, the broadening of the spectra, particularly around the exciton resonance, is insufficient, as expected. Because the pump pulse induced broadening is too small in comparison to the gap shift one gets at early negative delay times below the exciton resonance a small spectral range with positive DTS signal that is not observed in the experiment.

The effect of the energy relaxation due to LO-phonon scattering can be seen in detail in Fig. 4, which shows the resulting differential transmission spectra at three values of the delay time with time-dependent screened Coulomb scattering alone (full lines) and with additional LO-phonon scattering (dashed lines). Particularly at later delay times, it is obvious how the additional LO-phonon scattering allows a more efficient relaxation of the electrons into the energetically lower states.

While our previous analysis<sup>6</sup> with bare Coulomb potential scattering required short delay times and relatively low densities, our present model has no such limitations and allows one to calculate also the differential transmission spectra for stronger pump pulses. As an example we present in Fig. 5

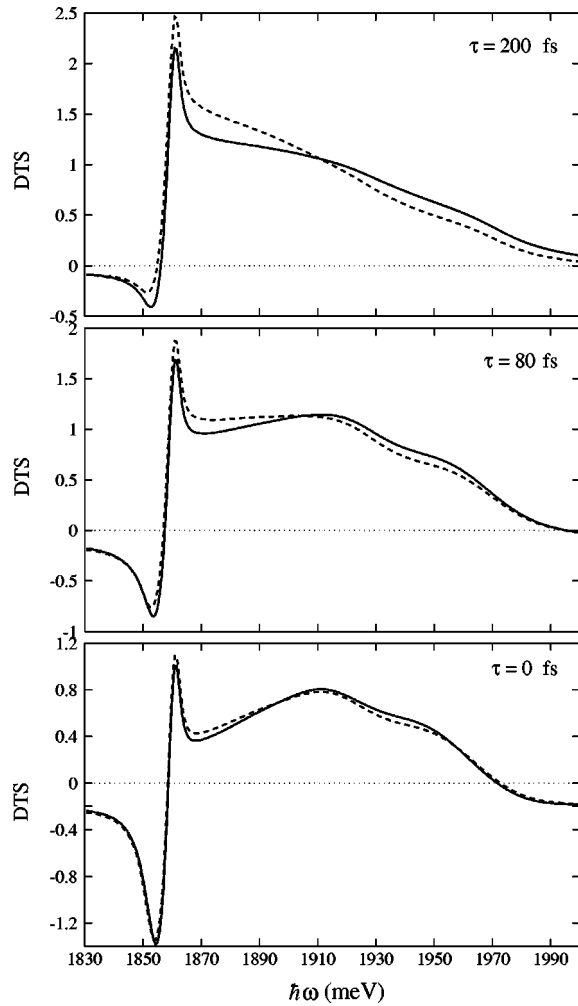


FIG. 4. Calculated differential transmission spectra for GaAs at 15 K for three delay times for the same parameters as in Fig. 3 with time-dependent screened Coulomb scattering only (full lines) and with both Coulomb and phonon scattering (dashed lines).

measured and calculated spectra with a pump pulse strength of  $\chi=1.34$  with a detuning of 50 meV, which excites an electron density of  $8.5 \times 10^{17} \text{ cm}^{-3}$ . For the calculation of the test spectra we used  $T_2^0=150 \text{ fs}$  and  $\gamma=0.4 \times 10^{-20} \text{ cm}^3 \text{ fs}^{-1}$ . A comparison with Fig. 3 shows that the spectra at later delay times changed from a triangular shape to a more squarelike shape due to the more degenerate electron distribution. The calculated spectra follow these general trend quite well. In particular, both the measured and the calculated spectra show the filling of states with increasing delay. One can follow this effect by watching the high-energy crossover to induced absorption above the filled state

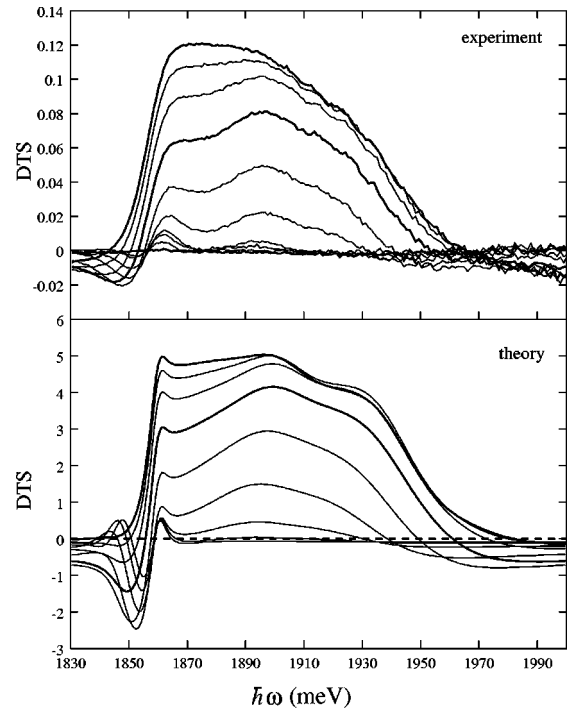


FIG. 5. Measured and calculated differential transmission spectra for GaAs at 15 K for various delay times in steps of 40 fs ranging from  $\tau=-200$  to 160 fs for a pump pulse with a strength of  $\chi=1.34$ , which generates the electron density  $n=8.5 \times 10^{17} \text{ cm}^{-3}$ . The central pump frequency has been taken as 1.569 eV, which corresponds to a detuning with respect to the unrenormalized lh-hh band gap of  $\Delta=50 \text{ meV}$ . For the calculation of the test spectra we used  $T_2^0=150 \text{ fs}$  and  $\gamma=0.4 \times 10^{-20} \text{ cm}^3 \text{ fs}^{-1}$ .

due to excitonic enhancement. Experiment and theory agree again qualitatively very well with the exception that pump induced line broadening is again too weak by the used density-dependent but undelayed phenomenological dephasing time. Only a full quantum kinetic treatment also of the dephasing of the test pulse induced interband polarization could improve the agreement around the shifted exciton resonance. However, this task exceeds the capacity of the present-day computers.

#### ACKNOWLEDGMENTS

We acknowledge support by the DFG-Schwerpunktprogramm *Quantenkohärenz in Halbleitern*. One of us (Q.T.V) gratefully acknowledges support by the KAAD. We are grateful to R. Planel and V. Thierry-Mieg (Laboratoire de Microstructures et de Microélectronique, Bagnex, France) for providing us with the high-quality GaAs sample and to M. Joffre and D. Hulin for helpful discussions.

<sup>1</sup>J. Shah, *Ultrafast Spectroscopy of Semiconductors and Semiconductor Microstructures* (Springer, Berlin, 1996).  
<sup>2</sup>H. Haug and A. P. Jauho, *Quantum Kinetics in Transport and Optics of Semiconductors* (Springer, Berlin, 1996).  
<sup>3</sup>L. Bányai, D. B. Tran Thoai, E. Reitsamer, H. Haug, D. Steinbach, M. U. Wehner, M. Wegener, T. Marschner, and W. Stolz,

Phys. Rev. Lett. **75**, 2188 (1995).

<sup>4</sup>M. U. Wehner, M. H. Ulm, D. S. Chemla, and M. Wegener, Phys. Rev. Lett. **80**, 1992 (1998).

<sup>5</sup>K. El Sayed, S. Schuster, H. Haug, F. Herzel, and K. Henneberger, Phys. Rev. B **49**, 7337 (1994).

<sup>6</sup>F. X. Camescasse, A. Alexandrou, D. Hulin, L. Bányai, D. B.

- Tran Thoai, and H. Haug, Phys. Rev. Lett. **77**, 5429 (1996).
- <sup>7</sup>P. Lipavský, V. Špička, and B. Velický, Phys. Rev. B **34**, 6933 (1986).
- <sup>8</sup>L. Bányai, Q. T. Vu, B. Mieck, and H. Haug, Phys. Rev. Lett. **81**, 882 (1998).
- <sup>9</sup>G. D. Mahan, *Many-Particle Physics* (Plenum, New York, 1981).
- <sup>10</sup>H. Haug and S. W. Koch, *Quantum Theory of the Optical and Electronic Properties of Semiconductors*, 3rd ed. (World Scientific, Singapore, 1994).
- <sup>11</sup>A. Alexandrou, V. Berger, and D. Hulin, Phys. Rev. B **52**, 4654 (1995).
- <sup>12</sup>*Numerical Data and Functional Relationships in Science and Technology*, edited by O. Madelung, Landolt-Börnstein, New Series, Group III, Vol. 17, Pt. a (Springer, Berlin, 1982).
- <sup>13</sup>J. L. Oudar, D. Hulin, A. Migus, A. Antonetti, and F. Alexandre, Phys. Rev. Lett. **55**, 2074 (1985).
- <sup>14</sup>W. H. Knox, C. Hirlimann, D. A. B. Miller, J. Shah, D. S. Chemla, and C. V. Shank, Phys. Rev. Lett. **56**, 1191 (1986).
- <sup>15</sup>W. Z. Lin, R. W. Schoenlein, J. G. Fujimoto, and E. P. Ippen, IEEE J. Quantum Electron. **24**, 267 (1988).
- <sup>16</sup>J.-P. Foing, D. Hulin, M. Joffre, M. K. Jackson, J.-L. Oudar, C. Tanguy, and M. Combescot, Phys. Rev. Lett. **68**, 110 (1992).
- <sup>17</sup>S. Hunsche, H. Heesel, A. Ewertz, H. Kurz, and J. H. Collet, Phys. Rev. B **48**, 17 818 (1993).
- <sup>18</sup>A. Leitenstorfer, C. Fürst, A. Laubereau, W. Kaiser, G. Tränkle, and G. Weinmann, Phys. Rev. Lett. **76**, 1545 (1996).
- <sup>19</sup>C. Fürst, A. Leitenstorfer, A. Laubereau, and R. Zimmermann, Phys. Rev. Lett. **78**, 3733 (1997).
- <sup>20</sup>S. Bar-Ad, P. Kner, M. V. Marquezini, D. S. Chemla, and K. El Sayed, Phys. Rev. Lett. **77**, 3177 (1996).
- <sup>21</sup>T. Elsaesser, J. Shah, L. Rota, and P. Lugli, Phys. Rev. Lett. **66**, 1757 (1991).
- <sup>22</sup>D. W. Snoke, W. W. Rühle, Y.-C. Lu, and E. Bauser, Phys. Rev. Lett. **68**, 990 (1992); Phys. Rev. B **45**, 10 979 (1992).
- <sup>23</sup>P. C. Becker, H. L. Fragnito, C. H. Brito Cruz, R. L. Fork, J. E. Cunningham, J. E. Henry, and C. V. Shank, Phys. Rev. Lett. **61**, 1647 (1988).
- <sup>24</sup>F. X. Camescasse, A. Alexandrou, and D. Hulin, Phys. Status Solidi B **204**, 293 (1997).
- <sup>25</sup>A. Alexandrou, V. Berger, D. Hulin, and V. Thierry-Mieg, Phys. Status Solidi B **188**, 335 (1995).